Homologous self-organising scale-invariant properties characterise long range species spread and cancer invasion

Diana E. Marco[1], Sergio A. Cannas[2], Marcelo A. Montemurro[3], Bo Hu[4, 5] and Shi-Yuan Cheng[4, 6]

[1]Laboratorio de Ecología Matemática, Area de Producción Orgánica, Facultad de Ciencias Agropecuarias, Universidad Nacional de Córdoba, Ciudad Universitaria, CC 508, 5000 Córdoba, Argentina. [2]Facultad de Matemática, Astronomía y Física, Universidad Nacional de Córdoba, Ciudad Universitaria, 5000 Córdoba, Argentina. [3] Faculty of Life Sciences University of Manchester, Jackson's Mill, G7, PO Box 88, Sackville St, Manchester, M60 1QD, United Kingdom.University of Pittsburgh [4]Cancer Institute & Department of [5]Medicine and [6]Pathology, Research Pavilion at the Hillman Cancer Center, Suite 2.26, 5117 Centre Avenue, Pittsburgh, PA 15213-1863, USA.

The invariance of some system properties over a range of temporal and/or spatial scales is an attribute of many processes in nature[1], often characterised by power law functions and fractal geometry[2]. In particular, there is growing consensus in that fat-tailed functions like the power law adequately describe long-distance dispersal (LDD) spread of organisms [3,4]. Here we show that the spatial spread of individuals governed by a power law dispersal function is represented by a clear and unique signature, characterised by two properties: A fractal geometry of the boundaries of patches generated by dispersal with a fractal dimension D displaying universal features, and a disrupted patch size distribution characterised by two different power laws. Analysing patterns obtained by simulations and real patterns

from species dispersal and cell spread in cancer invasion we show that both pattern properties are a direct result of LDD and localised dispersal and recruitment, reflecting population self-organisation.

Long-distance dispersal (LDD), even if represented by rare events, is one of the main factors explaining the fast spread of different organisms in new habitats, for example in paleocolonisation events[5], plant pathogens[6], and invasive species[7]. Also, as cancer can be viewed as an ecological process[8], metastatic spread from primary tumours can be thought as a biological invasion from cancer cells spreading and invading new organs. Colonization begins with a single or few cells previously dispersed from the primary tumor[9], originating different clone lines that evolve independently across the new tissues and organs invaded[10] in a process we can consider as LDD. In spite of the remarkable similarity with species spread, at present no detailed mechanism has been proposed for an ecological interpretation of cancer spread. In this paper we show that the spread of cells in cancer invasion and of invasive species generates a similar patchy pattern characterized by fractal and power law scaling. Furthermore, we show that this common pattern originates from self-organized, homologous mechanisms driven by LDD.

Fat-tailed functions like the power law seem to adequately describe LDD[3], and evidence for this is coming from crop pathogens distributions determined experimentally[11] and from model simulations[4,12]. Power law functions and fractal geometry characterise different ecological processes[1,2] as well as tumour growth[13,14], and they reflect the

invariance of some property over a range of temporal and spatial scales. There is increasing consensus in that they can be a byproduct of self-organising processes of populations and communities[15, 16]. Although the capacity of a system to evolve to an organised state due to intrinsic mechanisms, i.e., self-organisation, often characterised by a scale free selective geometry, has been attributed to diverse natural phenomena[17], the fundamental dynamics that determine its scaling properties have remained obscure in many cases. Performing independent simulations we show that the pattern properties we found in real data from cancer invasion and species spread are specific of long range dispersal mediated by a power law distribution function.

We performed simulations using a spatially explicit, individual-based model based on a cellular automaton originally developed for the study of biological invasions [18,19]. We simulated long ranged dispersal mechanisms using the power law dispersal function:

$$f(r)=\begin{cases}\dfrac{A}{r^{\alpha}} & if \quad r \geq 1/2 \\ 0 & if \quad 0<r<1/2\end{cases}$$

where A is a normalisation constant, r is the distance to the parental individual as $r=\sqrt{x^2+y^2}$ and $\alpha > 2$, as previously described[4]. The main biological significance of the inclusion of the power law as dispersal function is that dispersion is allowed to reach the whole area considered without distance limits. This is drastically different respect to the use of distribution functions allowing only short-distance dispersal (SDD), where dispersion can reach just close areas to the initial focus[4]. Also, the power law function allows for the inclusion of SDD and LDD events in the same dispersal function, depending on the value

of the α exponent[4]. According to the values of α of the LDD power law, when $3 < \alpha \leq 4$ the first moment (the mean) remains finite but the second moment (the variance) becomes infinite. The mean dispersal distance is given by $d \equiv < r > = (\alpha - 2) / 2 (\alpha - 3)$. When $2 < \alpha \leq 3$ both first and second moments are infinite, and thus the mean dispersal distance is not defined. Finally, for $\alpha > 4$ both the first and the second moments of the distribution are finite. Qualitative similar behaviour can be expected in the global spatial pattern of spread between this last case and SDD[20-23].

To characterise the spatial pattern of spread produced by the simulations, we calculated the mean fractal dimension *D* of patch borders using a box counting algorithm[24], and determined the patch size distribution. We analysed the spatial pattern produced by the model jointly with the patterns of spread of an LDD invasive tree (English elm, *Ulmus minor* Mill.) and cells from an invasive human glioma. We recorded the spread of English elm into a native forest from an initial small focus using aerial photographs taken in 1970, 1987 and 1996. Fruits of English elm are dispersed by wind (usually assumed to be a LDD mechanism) in high numbers but many seeds remain near the parent providing also SDD. We also analysed the spread of human glioma U87MG cells engineered to express an angiogenic regulator, angiopoietin-2 (Ang2) (U87MG/Ang2 cells), capable of promoting glioma cell infiltration into the brain parenchyma, established by intracranial xenografts in the brain of mice[25]. Invasion of glioma cells involves the attachment of invading tumour cells to extracellular matrix and disruption of matrix components, and subsequent cell penetration into adjacent brain structures. This process is mediated by tumour-secreted enzymes called matrix metalloproteases (MMPs) that degrade the extracellular matrix at tumour-invasive borders and invasive areas[25].

The analysis of pattern generation process with LDD during the simulations allows understanding its mechanism (**Fig. 1a, Movie S1**), which is essentially different from SDD mechanism (**Movie S2, 9, 17 Fig. 2a**). In LDD, beginning with an initially reproductive individual, a single patch appears surrounded by isolated, immature individuals (green dots, **Movie S1**) scattered all over the field (not shown). At times longer than the age of first reproduction, some of the scattered individuals begin reproduction (black dots, **Movie S1**), and secondary foci initiate growth into patches showing the same structure as the initial patch. While patches of higher order generation continue arising and growing, the first patch itself continues growing and absorbing the nearest patches. This coalescence of similar patches originates a self-similar border in the initial patch and it accounts for sudden increments in patch area. The same process of patch growth and coalescence occurs in other patches distant form the main patch. There is no a clearly defined invasion front **(Movie S1; Fig. 1a)**, and the spatial extent of the population grows exponentially (**Movie S1**). The spatial pattern of spread of English elm from aerial photographs resembled closely the pattern obtained by simulations (**Fig 1b**). The temporal and spatial patterns of patch generation from the initial focus composed by a small patch present in 1970 explain the resulting similarities (not shown). The number of patches initially grew exponentially and then slowed down. In 1987, about 74 new patches covered a small fraction of the area and were mainly represented by individual trees scattered through the 7 hectares forest area. The increase in covered area was also exponential although faster and continued, with 189 patches present ten years later. The faster area growth rate reveals that after a certain time, few new patches are generated but the increase in area is mainly due to patch growth and

coalescence, as occurred in the simulations. In agreement with simulations and species dispersion results (**Fig. 1a,b**), spread of the invasive, Ang2-expressing gliomas displayed irregular borders with spike-like structures that invaded into the normal brain structures (**Fig. 1c**), in contrast with the non invasive control tumours showing smooth, clean borders[25], clearly resembling the SDD process[4] (Movie S2). Glioma cells migrated far away the initial tumour and formed groups of individual tumour clusters that localized at 2.5–4.3 mm from the tumour mass in various invasive tumours, resembling the simulated pattern. Although it is not possible to image cell spreading in the brain tissue of mice in the *in vivo* model at sequential times, *in vitro* assays assessing the invasiveness of various glioma cells through membranes coated with Matrigel showed that U87MG/Ang2 cells had a 4-fold increase in invaded area compared with the parental U87MG cells[25], suggesting exponential increase.

The fractal dimension D of patch borders from simulations as a function of α varied between 1.6 and 1.7 for $2 < \alpha \leq 3$, and it decreased monotonously for $3 < \alpha \leq 4$. We calculated the fractal dimension D of patch borders from the digitised aerial images of English elm field cover in 1996. For the main field patch we found $D = 1.66$ ($R^2 = 0.93$, n = 10). Several of the remaining biggest patches showed D values ranged between 1.40 and 1.75 (R^2 between 0.95 and 0.99, n = 10 in all cases). These values correspond to predicted power law α exponents for LDD distribution functions[4]. In particular, $D = 1.66$ corresponds to $2 < \alpha \leq 3$, and thus the mean dispersal distance is not defined. An infinite mean in the basic interactions has been observed in diverse systems, and usually implies mean field behaviour[20-23]. This indicates that each individual virtually interacts with an average environment. Systems showing mean field behaviour present a high degree of universality,

that is, it is expected that most of the global properties will not depend on field details, such as habitat heterogeneity. This seems to be the case for the English elm spread, since wind dispersion ensures seeds reaching the whole area available as an extreme case of LDD. The fractal dimension of main tumour border calculated from the human glioma invasion was $D = 1.30$ ($R^2 = 0.99$, n = 16). This value corresponds again to predicted power law α exponents for LDD, although to $3 < \alpha \leq 4$ and thus the mean dispersal distance is defined[4]. This is in agreement with the mechanism of glioma cells dispersion, requiring the action of MMPs disintegrating the surrounding extracellular matrix to allow for cell migration and further dispersion along the tumour vessels. This process would set some constraints to the unrestricted LDD allowed by the power law function. Thus, the fractal D value of the patch borders generated by LDD provides information about the degree of interaction of the spreading organism with the surrounding environment.

We calculated the patch size distribution $P(s)$ excluding the initial patch from the simulations with LDD for a first reproductive age = 7 years and $\alpha = 3.33$. Patch size is calculated as the number of sites in each patch. $P(s)$ showed a disrupted distribution characterised by two different power laws $P(s) \sim s^{-\beta}$ at small and large patch areas s separated by a crossover region (**Fig. 2a)**. β value in the small patch areas was 3.37 ($R^2 = 0.98$), while in the large patch areas was 2.24 ($R^2 > 0.98$). Simulations using different values of α produced $P(s)$ curves with similar characteristics (not shown). Tracking individuals in the simulations we determined that the small area section of $P(s)$ is generated by random dispersal and aggregation of reproductively immature individuals. The large area section corresponds to larger patches generated by reproduction of previously dispersed individuals by LDD forming their own patches by localised dispersal

and recruitment through a founder effect, followed by growth and coalescence of neighbouring patches. Large area patches arise only at times greater than first reproduction (**Movie S1**). The average minimum area of patches generated by a single individual after its first reproductive event, corresponding to localised dispersion and recruitment, is $s^* = 65 \pm 5$ sites ($\ln (s^* \approx 4.2)$). These patches, that can be seen in the snapshot from **Fig.1a** and **Movie S1** as small patches with only one reproductive individual, are located at the beginning of the power law corresponding to large patch areas in the $P(s)$ curve (**Fig. 2a**). The English elm field $P(s)$ curve (**Fig. 2b)** closely resembled the $P(s)$ curves from simulations. Two power laws appear characterising the two sections of the curve, with $\beta = 3.27$ ($R^2 = 0.99$, n = 109) for the patches with small area and $\beta = 1.48$ ($R^2 = 0.88$, n =11) for patches with large areas. We determined s* for English elm as the s value corresponding to the point at the beginning of the second part of the $P(s)$ curve, and found $s^* = 90$ m^2 ($\ln (s^* = 4.5)$) (**Fig. 2b**). This s^* value is 3.6 times higher than the minimum field estimated canopy cover of an individual tree at first reproduction and thus compatible with a young patch originated by reproduction from a patch founder parent, followed by localised dispersal given by the SDD component. The scaling pattern of $P(s)$ is remarkable similar to the simulated pattern. $P(s)$ obtained for the glioma invasion (**Fig. 2c**) was very similar to the simulated and English elm patterns. The small and large area power laws show $\beta = 1,87$ ($R^2 = 0.97$, n = 4), and $\beta = 1,58$ ($R^2 = 0.95$, n = 6), respectively. Remarkably, again s* is located around ln 4, and its value (60 μm^2, ($\ln (s^* = 4.1)$), is compatible with a cluster of approximately 8 cells, indicating the early initiation of a microtumour by localised reproduction from a previously migrated cell. In a similar process, migrated cells of C6

glioma-astrocytoma originated multiple cell groups by division that appeared to be progenitors of tumour masses on Matrigel experiments[26].

The finding of distinctive fractal and scaling signatures of LDD in the spatial patterns generated by our simulations and their clear counterparts in the real patterns represents a significant step in the understanding of long range dispersal mechanisms in apparently diverse systems in nature. We showed that this mechanism of spread originates the spatial patterns of spread of an invader species and cancer cells. It is this similar origin what explains the similarity in pattern features by homology. Specifically, we now know in detail how the LDD process of spread can generate a fractal pattern by patch growth and coalescence, and how a disrupted patch size distribution appears by combination of LDD and localised dispersal and recruitment. For example, the process of patchy pattern generation we described supports the conjecture of LDD paleocolonisation of oak populations occurred 10,000 years ago[5]. The existence of patches which are virtually fixed for a single haplotype of chloroplast DNA scattered over several hundred square kilometers[5] can be explained by the LDD process of pattern generation through the founder effect we found. This founder effect is central to the clonal nature of cancer [10], and addresses important questions about clones expansion and control[8,27]. the mechanism of LDD we describe enlightens the present knowledge about the primary tumour growth and early metastatic spread. New cell lines disperse far away at very early times from the primary tumor and give early origin to clonal metastatic tumors with resistant characteristics through the founder effect we described. In particular, it is relevant to the

arising of resistant cell lines during metastatic invasion that challenges the traditional therapeutical approaches[26].

The LDD signature we found is robust since it depends only on the internal population dynamics and dispersal, reflecting self-organising processes. It appears that it is not fundamentally affected by other ecological processes like competitive interactions and habitat heterogeneity, since we found similar results from the single species, homogenous habitat modelling approach and from the complex field scenario involving the competitive spread of a species into a mountainous forest community[18] and from spread of cancer cells involving interaction with tumour microenvironment[25]. A minor variation appears in the fractal dimension of patch borders in relation to the dispersal environment, from high D values for the unrestrictive environment (simulation field) to medium and lower values to progressively restrictive environments (native forest and extracellular matrix). In addition, LDD pattern signature is robust to the spatial resolution level of analysis: while the model resolution is maximal (all individuals including newly born ones were traced in the simulations), resolution of real data is lower (only individuals of a minimum detectable size were recorded from the aerial images and cancer cell recognition depended on threshold detection in stained samples).

The choice of the adequate dispersal distribution function, the power law allowing extremely LDD and local subsequent dispersal and recruitment, was crucial both to obtain a sensible and realistic model output and to gather detailed explanation on the dynamics of LDD spread. Utilisation of bounded or partially bounded distribution functions in modelling LDD process has led to difficulties both in the predictive and explanatory aspects of the models. For example, the use of exponentially bounded dispersal functions

for modelling the spread of an invasive moth rendered discrepancies between the observed invasion rates, spatial pattern configuration and fractal characterisation[7,28]. In another example, the introduction of a hypothesised chemotactic attraction in a model of brain was necessary to produce a limited cell dispersion around the primary tumour in the simulations[29]. In particular, patterns generated by these models did not reflect the spread of the invasive individuals through a large area at very early invasion times. In the case of cancer, early detection is pivotal to improve its treatment or even cure it. Cancers detected at advanced stages are far more likely to cause death than those detected when while the cancer is still confined to the organ of origin[30]. Understanding and interpreting the process of cancer invasion in terms of long-range dispersal ecological mechanisms can help to understand the mechanisms of cancer spread and to develop more effective therapeutical strategies.

More generally, the self-organising, scale-invariant LDD features we found for species and cancer spread are especially relevant to biological invasions, epidemics and spread of genetically modified organisms, allowing the understanding of the mechanisms of spread of potentially harmful organisms.

Methods

The model, numerical simulations and spatial pattern analysis

We implemented the model as previously described[4,16,17]. Each site contains in the simulation field at most one individual. At every time step, empty sites are occupied wtih a probability that depends on the distribution of sites already occupied by mature individuals;

the contribution of those sites to the colonization probability is determined by the power law dispersal function allowing for LDD, as described in [4]. Simulations began with a single mature individual located at the centre of a square area. Spatial pattern analysis of species spread is based on the statistics of patches of occupied sites and their borders. At a fixed time occupied sites are assigned to patches by giving them a label, representing their corresponding patch number. When an unlabelled occupied site is found, the algorithm creates a new patch by assigning a new label to the current site and to all the connected set of occupied sites associated to it. For each site currently in the cluster all the occupied sites in the set of 8 closest sites are assigned to the same patch. The algorithm continues recursively until no more sites are added to the current patch. The procedure is repeated until no unlabelled occupied sites are left. A patch is then defined as a label that contains more than one site. The border set of a given patch is defined as the list of all the occupied sites lying at its border. For calculating D, we plotted the number of boxes $N(l)$ of linear size l as a function of l; the fractal dimension is defined as $N(l) \propto l^{D}$. We calculated the mean fractal dimension D of the patch borders as a function of time, where the averages were taken at fixed times over several simulation runs. We calculated the relative frequency histogram $P(s)$ of patches with size s (excluding the main patch), in an area of 1024 sites at the time when less than 50% of the sites were occupied. After this time the initial patch filled most of the simulation area and few isolated patches remained near the borders of the simulation area. Patch size is defined by the number of sites in each patch.

Field species data

We studied the spatial pattern of spread of English elm using aerial photographs from a forest area of 7 hectares located in a low mountain region of central Argentina. Native forest has been invaded by non-native, competing trees like English elm, Glossy privet (*Ligustrum lucidum*) and Honeylocust (*Gleditsia triacanthos*)[16]. English elm is a European tree introduced as ornamental species in the region around the mid 20th century. Reproduction is by seeds. We found no evidence of vegetative reproduction in the field. Individuals bear hermaphrodite flowers. Fruits are samaras released in high numbers and dispersed by wind. Black and white photographs were taken in 1970 (1: 5000), 1987 (1: 20 000), and 1996 (1: 5000). Photographs were digitised and interpreted using image processor software, identifying trees at an individual level. Photographs edges were not used in the interpretation to avoid image distortion. An estimation of error in the photograph interpretation was made by identifying individual trees in the photograph and then checking if they were correctly assigned to the species. In 97 % of cases assignments were correct. In 1970 there were only two near patches of few trees planted, considered as the first dispersal focus in the studied area. Number and area covered of patches generated from the first focus were calculated for 1987 and 1996, and the fractal dimension of patch borders was calculated using the box-counting method.

Cancer invasion data

Ang2-promoted human glioma invasion in the brain of animals were determined as described previously[23]. Briefly, U87MG Ang2-expressing cell clones (5×10^5) were stereotactically implanted into individual nude mouse brains with 5 mice per group. When mice developed neurological symptoms due to disturbance of their central nervous system,

mice were sacrificed and their brains were removed, processed and analyzed. The distance of invading glioma cells from tumour masses were assessed by capturing serial images of hematoxylin/eosin-stained brain sections using a Olympus BX51 (Melville, NY) microscope equipped with a SPOT digital camera (Diagnostic Instruments, Inc., Sterling height, MI) and calculated by the fact that under a 100 X magnification, one frame is equal to 1 mm long. Photographs were digitised and interpreted using image processor software, identifying cells at an individual level. Number and area covered for invasive cell clusters generated from the primary tumour were calculated and the fractal dimension of patch borders was calculated using the box-counting method.

1. Hastings, H. M. & Sugihara, G. *Fractals, a User´s Guide for the Natural Sciences*. (Oxford University Press, Oxford, 1993).
2. Enquist, B. J., Brown, J. H. & West, G. B. Allometric scaling of plant energetics and population density. *Nature* **395**, 163-165 (1998).
3. Kot, M., Lewis, M. A. & van den Driessche, P. Dispersal data and the spread of invading organisms. *Ecology* **77**, 2027-2042 (1996).
4. Cannas, S. A., Marco, D.E. & Montemurro, M. Long range dispersal and spatial pattern formation in biological invasions. *Math. Biosci.* **203**, 155–170 (2006).
5. Petit, R., Pineau, E., Demesure, B., Bacilieri, R., Ducousso, A. & Kremer, A. Chloroplast DNA footprints of postglacial recolonization by oaks. *Proc. Natl. Acad. Sci. USA* **94**, 9996-10001 (1997).

6. Brown, J. K. M. & Hovmoller, M. S. Aerial dispersal of pathogens on the global and continental scales and its impact on plant disease. *Science* **297**, 537-541 (2002).

7. Gilbert, M., Grégoire, J. C., Freise, J. F. & Heitland, W. Long-distance dispersal and human population density allow the prediction of invasive patterns in the horse chestnut leafminer *Cameraria ohridella*. *Ecology* **73**, 459–468 (2004).

8. Merlo, L.. M. F., Pepper, J. W., Reid, B. J. & Maley, C. C. Cancer as an evolutionary and ecological process. *Nature Rev. Cancer* **6**, 924-935 (2006).

9. Talmadge, J. E., Wolman, S. R. & Fidler, I. J. Evidence for the clonal origin of spontaneous metastases *Science* 217: 361-363 (1982).

10. Nowell, P. C. The clonal evolution of tumour cell populations. *Science* **194**, 23–28 (1976).

11. Gibson, G. J. Investigating mechanisms of spatio-temporal epidemic spread using stochastic models. *Phytopathology* **87**, 139–146 (1997).

12. Shaw, M. W. Simulation of population expansion and spatial pattern when individual dispersal distributions do not decline exponentially with distance. *Proc. R. Soc. Lond. B Biol. Sci.* **259**, 243-248 (1995).

13. Brú, A., Pastor, J. M., Fernaud, I., Brú, I., Melle, S. & Berenguer, C. Super-Rough Dynamics on Tumour Growth. *Phys. Rev. Lett.* **81**, 4008-4011 (1998).

14. Hart, D., Shochat, E. & Agur, Z. The growth law of primary breast cancer as inferred from mammography screening trials data. *Br. J. Cancer* **78**, 382-387 (1998).

15. Sutherland, B. R. & Jacobs, A. E. Self-organization and scaling in a lattice predator–prey model. *Complex Systems* **8**: 385–405 (1994).

16. Pascual, M., Roy, M., Guichard, F. & Flierl, G. Cluster size distributions: signatures of self-organization in spatial ecologies. *Phil. Trans. R. Soc. Lond. B* **357**, 657–666 (2002).

17. Mandelbrot, B. B. *The Fractal Geometry of Nature* (W. H. Freeman, San Francisco, 1982).

18. Marco, D. E., Paez, S. A. & Cannas, S. A. Species invasiveness in biological invasions: a modelling approach. *Biol. Inv*. **4**, 193-205 (2002).

19. Cannas, S. A., Marco, D. E. & Paez, S. A. Modelling biological invasions: species traits, species interactions and habitat heterogeneity. *Math. Biosci*. **183**, 93-110 (2003).

20. Cannas, S. A. & de Magalhães, A. C. N. The one-dimensional Potts model with long-range interactions: arenormalization group approach. *J. Phys. A: Math. Gen*. **30**, 3345-3361 (1997).

21. Cannas, S.A. Phase diagram of a stochastic cellular automaton with long-range interactions. *Physica A* **258**, 32-44 (1998).

22. Gleiser, P. M., Tamarit, F. A. & Cannas, S. A. Self-organized criticality in a model of biological evolution with long-range interactions. *Physica A* **275**, 272-280 (2000).

23. Gleiser, P. M., Cannas, S. A., Tamarit, F. A. & Zheng, B. Long-range effects in granular avalanching. *Phys. Rev. E* ***63***, 042301 (2001).

24. Halley, J. M. *et al.* Uses and abuses of fractal methodology in ecology. *Ecol. Lett.* **7**, 254-271 (2004).

25. Hu, B., Guo, P., Fang, Q., Tao, H., Wang, D., Nagane, M., Huang, H. S., Gunji, Y., Nishikawa, R., Alitalo, K., Cavenee, W. K. & Cheng, S. Angiopoietin-2 induces human glioma invasion through the activation of matrix metalloprotease-2. *PNAS* **100**, 8904–8909 (2003).

26. Bernstein, J. J., Laws, E. R. Jr, Levine, K. V., Wood, L. R., Tadvalkar, G. & Goldberg, W. J. C6 glioma-astrocytoma cell and fetal astrocyte migration into artificial basement membrane: a permissive substrate for neural tumours but not fetal astrocytes. *Neurosurgery* **28**, 652-658 (1991).

27. Vargo-Gogola, T. & Rosen, J. M. Modelling breast cancer: one size does not fit all. *Nat. Phys.* **7**: 659-672.

28. Gilbert, M. et al. Forecasting *Cameraria ohridella* invasion dynamics in recently invaded countries: from validation to prediction. *J. Applied Ecol*. **42**, 805–813 (2005).

29. Sander, L. M. & Deisboeck, T. S. Growth patterns of microscopic brain tumours. *Phys. Rev. E* 66, 051901 (2002).

30. Etzioni, R. *et al.* The case for early detection. *Nature Rev. Cancer* 3: 1–10 (2003).

Supplementary Information is included.

Acknowledgements This research was supported by grants from Secyt-Universidad Nacional de Córdoba, Agencia Córdoba Ciencia and CONICET (Argentina), the Medical Research Council of the United Kingdom, the National Institute of Health, USA (CA102011), American Cancer Society, USA (RSG CSM-107144) and

the Hillman Fellows Program (S.-Y. C. and B. H.). D.E.M. and S.A.C. are members of the National Research Council (CONICET, Argentina).

Author information Reprints and permissions information is available at npg.nature.com/reprints and permissions. The authors declare that they have no competing financial interests. Correspondence and requests for materials should be addressed to D.E.M. (dmarco@agro.uncor.edu)

Figure Legends

Figure 1. Snapshots of long-distance dispersal (LDD) spread. a, Simulation spread from an individual in an area with L = 200 sites after 9 years from first reproductive time (7 years). Reproductive (black dots) and immature (grey dots) individuals are shown. Power law LDD with α = 3.11. **b**, Spatial spread of English elm (black areas) surrounded by a mixed forest of other invasive and native species (white ground). **c**, Spatial spread of human invasive glioma in (black areas) in mouse brain (white ground).

Figure 2. Size distribution of patches *P* (*s*). a, *P* (*s*) for LDD simulations for first reproductive age = 7 years and α = 3.33…*s* is given in number of sites. **b,** *P* (*s*) for field spread of English elm. *s* is given in m^2. **c**, *P* (*s*) for spread of human invasive glioma. s is given in μm^2. *P* (*s*) curves are characterised by power laws ($P(s) \sim s^{-\beta}$), corresponding to patches of small and large areas. *β* values are given in the text. *s** indicates the estimated average minimum size of a patch generated by a single individual by reproduction and localised dispersal in the simulations **a** and in real data **b, c**.

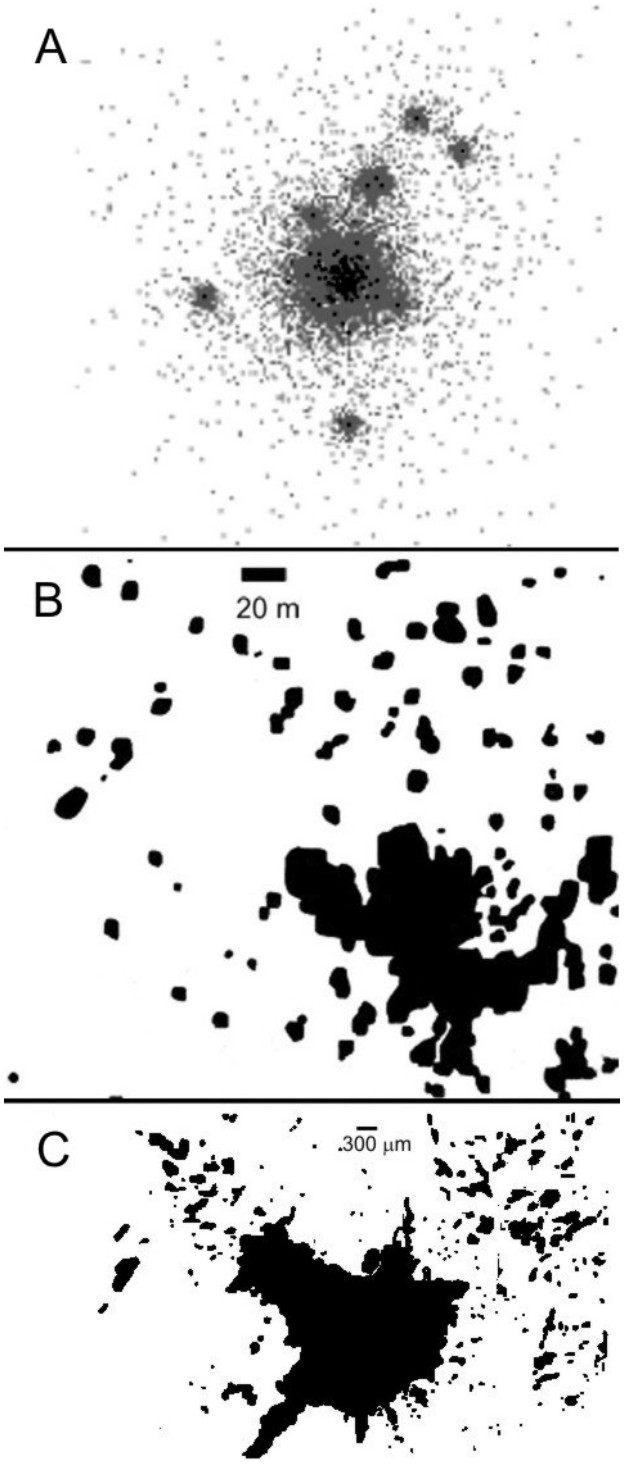

Fig. 1.

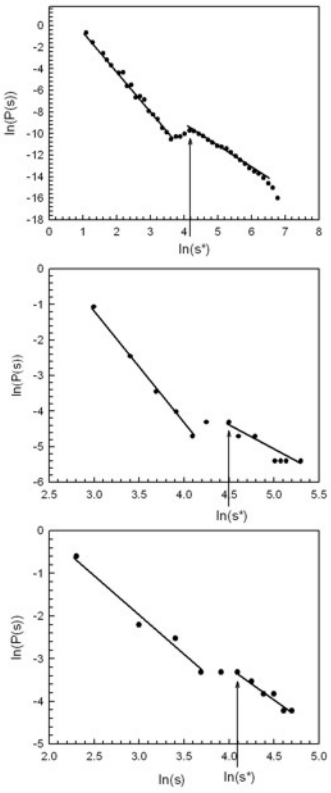

Fig. 2